Validation of an Integrated Estimation of Loblolly Pine (*Pinus taeda* L.) Leaf Area Index (LAI) Using Two Indirect Optical Methods in the Southeastern United States

John S. Iiames Jr., Russell Congalton, Andrew Pilant, and Timothy Lewis

ABSTRACT

Quality assessment of satellite-derived leaf area index (LAI) products requires appropriate ground measurements for validation. Since the National Aeronautics and Space Administration launch of Terra (1999) and Aqua (2001), 1-km, 8-day composited retrievals of LAI have been produced for six biome classes worldwide. The evergreen needle leaf biome has been examined at numerous validation sites, but the dominant commercial species in the southeastern United States, loblolly pine (*Pinus taeda*), has not been investigated. The objective of this research was to evaluate an in situ optical LAI estimation technique combining measurements from the Tracing Radiation and Architecture of Canopies (TRAC) optical sensor and digital hemispherical photography (DHP) in the southeastern US *P. taeda* forests. Stand-level LAI estimated from allometric regression equations developed from whole-tree harvest data were compared to TRAC–DHP optical LAI estimates at a study site located in the North Carolina Sandhills Region. Within-shoot clumping, (i.e., the needle-to-shoot area ratio [γ_E]) was estimated at 1.21 and fell within the range of previously reported values for coniferous species (1.2–2.1). The woody-to-total area ratio ($\alpha = 0.31$) was within the range of other published results (0.11–0.34). Overall, the indirect optical TRAC–DHP method of determining LAI was similar to LAI estimates that had been derived from allometric equations from whole-tree harvests. The TRAC–DHP yielded a value 0.14 LAI units below that retrieved from stand-level whole-tree harvest allometric equations. DHP alone yielded the best LAI estimate, a 0.04 LAI unit differential compared with the same allometrically derived LAI.

Keywords: LAI, TRAC, DHP, allometric, MODIS, general

The assessment of ecosystem condition through the satellite monitoring of terrestrial vegetation extent, biomass, and seasonal dynamics has begun to answer questions related to carbon sequestration and the expansion of greenhouse gases, biogenic emissions and their inputs into air quality, and other significant environmental issues. Leaf area index (LAI), defined here as one-half the total green leaf area per unit ground surface area (Chen and Black 1992a), has been indirectly linked to the estimation of terrestrial energy, carbon, water cycle processes, and biogeochemistry of vegetation, through the quantification of surface photosynthesis, evapotranspiration, and annual net primary production (Aber and Melillo 2001). LAI has been identified as the variable of greatest importance for quantifying energy and mass exchange by plant canopies over landscapes (Running and Coughlan 1988) and has been shown to explain 80–90% of the variation in the aboveground net primary production for forests in the United States (Gholz 1982, Gower et al. 1992, Fassnacht and Gower 1997). Appropriate field-measured LAI techniques are required to correlate satellite spectral values with in situ LAI values. The aim of this study was to evaluate an in situ optical LAI estimation technique for loblolly pine (L. *Pinus taeda*) in the southeastern United States. Results from this study will later aid in the assessment of an LAI product derived from the National Aeronautics and Space Administration Moderate-Resolution Imaging Spectrometer (MODIS) sensor aboard the Terra (1999) and Aqua (2002) Earth Observing System (EOS) spacecrafts.

The significance of LAI as source data for process-based ecological models has been well documented. Running and Coughlan (1988) ranked LAI as the most important attribute of vegetation structure for characterizing forest canopies over large areas at broad spatial scales using satellite remote sensing data. Leaves have been identified as the main surface of exchange between the plant canopy and the atmosphere and have been related to canopy light interception; evapotranspiration; net photosynthesis; and gas, water, carbon, and energy exchange (Hall et al. 2003). Gower et al. (1999) noted that most ecosystem process models that simulate carbon and

Received February 7, 2007; accepted January 18, 2008.

John S. Iiames Jr. (iiames.john@epa.gov), US Environmental Protection Agency, Landscape Characterization Branch, 109 TW Alexander Drive, MD E243-05, Research Triangle Park, NC 27612. Russell Congalton (russ.congalton@unh.edu), University of New Hampshire, Durham, NC 03824. Andrew Pilant (pilant.drew@epa.gov), US Environmental Protection Agency, 109 T.W. Alexander Dr. (MDE243-05), RTP, NC, 27711. Timothy Lewis (Timothy.e.lewis@erdc.usace.army.mil), US Army Corps of Engineers, Engineer Research and Development Center, 3909 Halls Ferry Rd., Vicksburg, MS, 39180. *The authors would like to thank Mr. Malcolm Wilkins for his development/construction of the pine-shoot imaging apparatus. We would also like to thank Dr. Lee Allen and Tim Albaugh from North Carolina State University for their input into this project. Also, Pete Anderson, with the United States Forest Service was especially helpful with location/access issues at the SETRES site. Sylvain Leblanc from the Canadian Center for Remote Sensing was very helpful with his review and input into indirect optical LAI measurement theory. Notice: The U.S. Environmental Protection Agency funded and conducted the research described in this paper. Although this work was reviewed by EPA and has been approved for publication, it may not necessarily reflect official Agency policy. Mention of any trade names or commercial products does not constitute endorsement or recommendation for use.*

hydrogen cycles require LAI as an input variable. Vegetation plays a vital role in global climate change by controlling terrestrial mass and energy fluxes (Oren et al. 2006). Interest in tracking LAI phenology is linked to the role forests play in the sequestration of carbon from carbon emissions (Johnsen et al. 2001) and the formation of tropospheric ozone from biogenic emissions of volatile organic compounds naturally released into the atmosphere (Geron et al. 1994).

LAI has been estimated from remote sensing satellites using empirical relationships between ground estimated LAI and vegetation indices derived from primary spectral bands, especially the red and the near-infrared wavelengths, taking advantage of the red-edge phenomenon existent within photosynthetically active vegetation. These sensors differ in spectral, spatial, radiometric, and temporal resolutions. Columbo et al. (2003) retrieved LAI over multiple vegetation types with high (spatial)-resolution imagery (IKONOS). A number of studies have estimated LAI using medium (spatial)-resolution imagery from both the Landsat Thematic Mapper (Hughes Santa Barbara Remote Sensing, Goleta, GA) (Chen and Cihlar 1996, Fassnacht et al. 1997, Weiss et al. 2001) and the SPOT high-resolution visible sensor (Weiss et al. 2001). Low spatial resolution sensors such as the Advanced Very High Resolution Radiometer (Gottschalck et al. 2002) and MODIS have produced LAI products at 8- and 1-km scales, respectively.

The development of appropriate ground sampling strategies is critical to the accurate specification of uncertainties in LAI products estimated from remotely sensed data (Tian et al. 2002). Errors produced in ground-derived measures of LAI are either additive or multiplicative. Issues of concern regarding in situ measurements of LAI for remote sensing validation include positional accuracy, spatial scale, and field sampling intensity (Hall et al. 2003). With the launch of the MODIS sensor aboard the Terra (1999) and Aqua (2002) EOS spacecrafts, LAI and the fraction of photosynthetically active radiation (PAR) have been estimated since early 2000 from the spectral and angular properties captured by these sensors. The MOD15A2 LAI product is a 1-km global data product composited over an 8-day period. This product is derived from a three-dimensional radiative transfer model that is driven by an atmospherically corrected surface reflectance product (MOD09), a land cover product (MOD12), and ancillary information on surface characteristics. The assessment and validation of this product (MOD15A2) in the evergreen needle leaf biome, one of six biomes delineated in the MOD12 land cover product is needed in the southeastern region of the United States. This article addresses the first step in the process of MOD15A2 validation, the assessment of accuracy and precision of LAI field estimates.

In situ LAI measurement methods include three measurement types: direct, semidirect, and indirect. Direct LAI measurement techniques are only applicable in forage or agricultural ecosystems where 100% of the vegetation in a defined area is harvested and measured. Larger-scale forested ecosystems require semidirect or indirect LAI estimation approaches. Semidirect LAI estimation techniques include (1) litterfall collection, where spatial and temporal sampling schemes are used to scale the data to the stand level, and (2) allometric regression equations developed from whole-tree destructive sampling. Allometry developed from destructive sampling is regarded as the most accurate LAI estimation approach, yielding the closest approximation of "true" LAI (Jonkheere et al. 2005). However, destructive sampling is time-consuming and labor-intensive, motivating the development of a more rapid in situ LAI estimation technique employing indirect optical methods. The goal of this study is to evaluate an in situ optical LAI estimation technique that combines the Tracing Radiation and Architecture of Canopies (TRAC) optical sensor and digital hemispherical photography (DHP) in southeastern US loblolly pine (*P. taeda*) forests. Stand-level LAI estimated from allometric regression equations developed from whole-tree harvest data was compared with TRAC–DHP optical LAI estimates at a study site located in the North Carolina Sandhills Region. The significance of accurate estimates of southern pine forest attributes (i.e., LAI) is important in accounting for local and regional carbon sequestration, atmospheric deposition, and biogenic emissions. The southern region accounts for 24% of the land area in the United States, of which 58% is forested. Of this forested land, 20% is owned by forest industry (Johnsen et al. 2001). In particular, the area of commercial forestlands in *P. taeda* has increased by 15.3% in 29 years from 1960 to 1989 (Schultz 1997). Because, regionally, *P. taeda* is a major component in understanding air quality and carbon sink/sources, an understanding of seasonal and annual LAI fluctuations is important.

Indirect Optical LAI Measurement Theory

Indirect optical methods for LAI estimation involve ground measurement of gap fraction defined as the percentage of gaps through the canopy that are estimated by direct or diffuse light transmittance through the canopy to the forest floor. These optical methods apply the Beer-Lambert Law (Beer 1853) that accounts for the total amount of radiation intercepted by a canopy layer dependent on the incident irradiance, canopy structure, and optical properties of the site (Jonckheere et al. 2005). The Beer-Lambert Law is expressed as

$$P(\theta) = e^{-G(\theta)\,L_e/\cos(\theta)}, \quad (1)$$

where θ is the zenith angle of view, $P(\theta)$ is the gap fraction defined as the probability of uncollided radiation penetration through the foliage at θ, L_e is the effective LAI, and $G(\theta)$ is the projection coefficient, a factor corresponding to the fraction of foliage area projected on the plane normal to the zenith direction. Effective LAI (L_e), i.e., a canopy attribute influenced by the "effect" of nonrandom foliage spatial distribution on indirect measurements of LAI, can be derived indirectly from this radiation inversion model (i.e., light extinction model) based on the probability (P) of a light ray missing all foliage elements while passing through a canopy at some angle θ. Assuming that canopy foliage elements exhibit a Poisson process (i.e., they are randomly distributed in the horizontal plane) it is possible to derive expressions for the 95% confidence limits of gap fraction.

Both optical sensors used in this study (TRAC and DHP) can extract gap fraction information from forest canopies. However, TRAC requires a continuous measurement of $P(\theta)$ between a zenith θ of 30 and 60° (usually one-half day) to determine a final gap fraction value. DHP measures gap fraction instantaneously over a wide range of zenith angles. An estimate of the projection coefficient $G(\theta)$ in the absence of known leaf angle distribution requires gap fraction measurements over the entire range of zenith angles (Miller 1967). However, at 1 radian (57.3°), the projection coefficient $G(\theta)$ approaches 0.5 because of the theoretical insensitivity of the $P(\theta)$ to leaf angle distribution at that angle (Wilson 1963, Jones 1992). The 1-radian criterion for $G(\theta)$ of 0.5 has been shown over a wide variety of leaf and needle structures. Leblanc and Chen (2001) observed a convergence point ($G(\theta) = 0.54$) within a clumped canopy at $\theta =$

62°, implying that a random foliage assumption near 60° is reasonable in estimating L_e. Also, an almost perfect fit ($R^2 = 0.99$) was found in the comparison between L_e retrieved from multiple angles when compared with L_e estimated from the 48–58° range (Leblanc and Chapman 2006). Therefore, a gap fraction determined from hemispherical photography at 1 radian may assume a projection coefficient of 0.5, eliminating the prior requirement of solving for this parameter over multiple angles.

Under the "random horizontal distribution of canopy foliage elements" assumption, effective LAI (L_e) can be retrieved with gap fraction measurements made from indirect optical sensors with an assumed projection coefficient $G(\theta)$ of 0.5. In nature, however, canopies are distributed nonrandomly (i.e., clumped) in the horizontal plane. The spatial distribution of foliage elements is dictated by distinct canopy architecture including stem distributions, crown form, whorls, branches, shoots, and groups of trees (Chen et al. 1997). Therefore, to account for the nonrandom foliage distribution within a forest stand, a correction factor, $\Omega(\theta)$, or total clumping index (Chen 1996), is needed to convert the randomly assumed effective LAI (L_e) to a nonrandom LAI, defined as L_t. The total clumping index is a parameter determined by the deviation of the spatial distribution of a vegetative canopy from a random case (LeBlanc and Fournier 2005). Thus, effective LAI (L_e) is decomposed into two components: total LAI (L_t) and total clumping index $\Omega(\theta)$,

$$L_e(\theta) = L_t \cdot \Omega(\theta). \quad (2)$$

Chen (1996) defined $\Omega(\theta)$ as

$$\Omega(\theta) = \frac{\Omega_E(\theta)}{\gamma_E}. \quad (3)$$

Ω_E quantifies the effect of foliage clumping at scales larger than the shoot, whereas γ_E represents the needle-to-shoot area ratio (i.e., one-half the needle area to one-half of the shoot silhouette area) quantifying within-shoot clumping (Fassnacht et al. 1994, Chen et al. 1997). The needle-to-shoot area ratio measurement is untenable with optical measuring devices because of the insensitivity of the sensors in resolving the small gaps found within conifer shoots. Thus, this parameter is extracted with field and laboratory measurements. The element clumping index Ω_E is quantified by measurements made with TRAC and DHP. A regular horizontal distribution of foliage dispersion yields a total clumping index of greater than 1.0, a random foliage distribution yields a value of 1.0, and clumped foliage distributions, typically found in coniferous forests, produce values less than 1.0 (Nilson 1971, Gower et al. 1999).

The total clumping index $\Omega(\theta)$ is assumed to be equal to unity (i.e., 1.0) with some optical instruments, e.g., the LiCOR Plant Canopy Analyzer (PCA; LI-COR Biosciences, Lincoln, NE). However, the element clumping index Ω_E, a component necessary for solving for $\Omega(\theta)$, can be generated from gap size distribution data retrieved from the TRAC and DHP sensors and processed by the gap removal method (Chen and Cihlar 1995b). The LiCOR PCA measures gap fraction but does not account for gap size distribution, resulting in an underestimation of LAI within coniferous forest stands where foliage is clumped at the shoot and canopy levels (Gower and Norman 1991, Fassnacht et al. 1994, Kucharik et al. 1998). LiCOR PCA underestimations of LAI within the conifer forest type assuming a random distribution of vegetation include 38% (Smith et al. 1993), 35–40% (Gower and Norman 1991), and 26.5% (Cutini et al. 1998). To solve for Ω_E, a gap accumulation curve is produced, with gap fraction accumulating from the largest to the smallest gap; and then a gap removal method is used to quantify gaps resulting from the nonrandom nature of the canopy (Chen and Cihlar 1995a). The element clumping effect Ω_E is then determined from the difference between measured gap fraction and gap fraction after removal of the gaps due to nonrandomness.

When assuming a random horizontal spatial distribution of canopy elements, L_e acquired in the coniferous forest type will be lower than actual LAI if not corrected for clumping at the shoot and the stand levels. However, L_e is affected not only by the canopy randomness assumption, but also by the proportion of nonphotosynthetic to photosynthetic materials apparent within the field of view of the optical sensor. All indirect optical sensors are incapable of differentiating green photosynthetic biomass from all other woody plant materials, thus making L_e a measurement of overall plant area. Therefore, a ratio of the nonphotosynthetic to photosynthetic material, defined as the woody-to-total area ratio (α), is required to correct L_e. Here, α is a ratio of the projected area of the wood to the total projected area. Integrating the corrections for clumping and the proportion of woody material within a canopy, Chen et al. (1997) modified the equation (i.e., modified Beer-Lambert light extinction model) to solve for true LAI as

$$\text{LAI} = (1 - \alpha) \cdot (L_e(\lambda_E/\Omega_E)), \quad (4)$$

In summary, the effective LAI (L_e), is estimated from hemispherical photography gap fraction measurements at 57.3°; the element clumping index Ω_E is calculated from gap size distributions determined from TRAC measurements; the woody-to-total area (α) and needle-to-shoot area ratios (γ_E) are calculated from a combination of field and lab methods.

Indirect Optical Instruments

Indirect in situ optical estimation methods of LAI rely on the measurement of gap fraction, i.e., the fraction of transmitted incident radiation through a plant canopy. These instruments can be divided into two categories dependent on the type of incident radiation received at the sensor, either direct or diffuse. The TRAC instrument detects direct solar irradiance at known solar angles along an established transect (Fournier et al. 2003), whereas the DHP makes use of diffuse light conditions recorded at specific locations.

TRAC

The TRAC sunfleck profiling instrument consists of three quantum PAR (400–700 nm) sensors (model LI-190SB; LI-COR, Lincoln, Nebraska), two uplooking and one downlooking, mounted on a wand with a built-in datalogger (Leblanc et al. 2002). The instrument is operated under direct sun conditions and is carried along a linear transect at a constant speed of 0.3 m s^{-1}. Typical transect lengths of 50–100 m or greater are oriented close to perpendicular to the direction of the sun and are marked in fixed intervals, typically 10-m subdivisions. A user-defined time stamp initiates the transect collection with each intermediate 10-m subdivision also marked by the user progressing along the transect. The instrument records the downwelling solar photosynthetic photon flux density (PPFD) from one of the uplooking sensors in units of micromoles (meter squared) per second at a sampling frequency of 32 Hz. The datalogger records light–dark transitions as the direct solar beam is alternately transmitted and eclipsed by canopy elements.

This record of sunflecks and shadows is processed to yield a canopy gap size distribution, a necessary component in the calculation of the element clumping index (Ω_e). TRACWin software (Leblanc et al. 2002) processes the Ω_e by determining the deviation of the measured gap size distribution from that of randomly distributed foliage (Morisette et al. 2006). TRACWin also produces an LAI estimate based on retrieved effective LAI (L_e) from user-defined inputs of a species-specific woody-to-total area ratio (α) and needle-to-shoot area ratio (γ_E). To arrive at an estimate of LAI, L_e is first estimated under the assumption of random foliage distribution by inverting the Beer-Lambert equation (Eq. 1). Leblanc et al. (2002), however, recommends integrating L_e retrieved from either hemispherical photography or the LiCOR PCA because the TRAC acquires this parameter at only one θ at the time of data acquisition. These two instruments (LiCOR PCA and hemispherical photography) are capable of capturing multiple gap fraction estimates over many θs from one data collection.

TRAC data quality is influenced by solar zenith and azimuth. Optimal results are achieved with a θ between 30 and 60°. As θ approaches the horizon ($\theta > 60°$), the relationship between LAI and light extinction becomes increasingly nonlinear. Similarly, best results are attained when TRAC sampling is conducted with a solar azimuth perpendicular to the transect azimuth. Sky condition is also an important factor for TRAC measurements. Clear sky with unobstructed sun is optimal. Overcast conditions are unsuitable; the method requires distinct sunflecks and shadows.

DHP

Photographs taken upward from the forest floor with a 180° hemispherical (fisheye) lens produce circular images that record the size, shape, and location of gaps in the forest overstory. A properly classified fisheye photograph provides a detailed map of sky visibility and obstructions (sky map) relative to the location where the photograph was taken. Various software programs, such as Gap Light Analyzer (GLA; Simon Fraser University, Burnaby, BC, Canada), Hemiview (Delta-T Devices, Cambridge, United Kingdom), WinSCANOPY (Regent Instruments, Inc., Quebec, QC, Canada), and DHP (Leblanc et al. 2005) are available to process film or digital fisheye camera images into a myriad of metrics that reveal information about the light regimes beneath the canopy and the productivity of the plant canopy. These programs rely on an accurate projection of a three-dimensional hemispherical coordinate system onto a two-dimensional surface. Accurate projection requires calibration information for the fisheye lens used and any spherical distortions associated with the lens. The calculation of canopy metrics depends on accurate measures of gap fraction as a function of zenith angle and azimuth. The digital image can be divided into zenith and azimuth "sky addresses" or sectors. Each sector can be described by a combined zenith angle and azimuth value. Within a given sector, gap fraction is calculated with values between 0 (totally "obscured" sky) and 1 (totally "open" sky) and is defined as the proportion of unobscured sky as seen from a position beneath the plant canopy.

Hemispherical analysis relies on the assumptions that the canopy above the photograph is a single layer and that all leaves completely obscure incoming solar radiation. However, potential error may be introduced in the classification of sky and no-sky regions because of unaccounted light transmission and reflection through and from the individual leaf. Canopy gaps existing in darker areas of the canopy also may be a result of the partial transmission of light through that portion of the canopy (Roxburgh and Kelly 1995).

Methods

Site Description

The TRAC–DHP indirect optical estimation technique was evaluated at the Southeast Tree Research and Education Site (SETRES), a site that is part of a *P. taeda* long-term nutritional study established by the North Carolina State Forest Nutritional Cooperative (NCSFNC; Figure 1). SETRES is located in the Sandhills of Scotland County, North Carolina (34.917°N, 79.500°W) and exists on a flat, infertile, excessively drained, sandy, siliceous, thermic Psammentic Hapludult soil from the Wakulla series (Soil Survey Division 2001). Annual precipitation averages 1,210 mm (30-year average), but extended droughts are possible during the growing season. Average annual temperature is 17°C (30-year average). The site was planted with *P. taeda* on a 2 × 3-m spacing in 1985 (Albaugh et al. 1998). In 1992 a long-term fertilization and irrigation experiment was established (Murthy and Dougherty 1997, Dougherty et al. 1998). Site index (meters at 25 years) was 16 for this site. Site index is a relative measure of forest site quality based on the height (meters) of the dominant and codominant trees in well-stocked, even-aged stands at a specific age.

Two plots, S1P (34.9024°N, 79.4862°W) and S2P (34.9011°N, 79.4886°W), were located in nontreatment areas (i.e., adjacent stands to treatment areas) with real-time differential global positioning systems (OMNISTAR) with a ±1-m horizontal accuracy. On both plots, three 100-m transects were laid along the following azimuths: 45, 90, and 135°, with all three transects intersecting at the plot center or 50-m mark of each transect (Figure 2). Each 100-m transect was marked every 10 m with flagging for TRAC measurement time marks. TRAC measurements were made along transects closest to perpendicular to the solar azimuth at sampling time between the θ of 30 and 60°. DHP measurements were located along each transect at the 10-, 50-, and 90-m marks and were made during diffuse light conditions (at dawn or dusk).

TRAC measurements were made only on S1P, whereas DHP measurements were made on both plots S1P and S2P. Measurements of forest structural attributes were made on three subplots at S1P using a 10-m radius fixed-area sampling method. All trees within this 10-m radius were tallied for species type, dbh of 1.4 m above tree base, and tree height (meters). *P. taeda* stocking for both plots averaged 1,770 trees ha^{-1} with a mean dbh of 14.5 cm. The average height of the dominant–codominant crown class was 12.3 m ($\sigma \pm 1.3$). Less than 3% of the SETRES site was composed of suppressed (less than 7.6-cm dbh) longleaf pine (*Pinus palustris*). Canopy closure, defined as the percent obstruction of the sky by canopy elements, was estimated at 77.5% using a Geographic Resource Solutions Densitometer (Ben Meadows Company, Janesville, Wisconsin). Deciduous hardwood understory was present with all stems less than 5-cm dbh.

Optical TRAC-DHP and Field Measurements

The following section presents the methods used to extract the parameters from Equation 4. In summary, the effective LAI L_e is estimated from hemispherical photography gap fraction measurements; the element clumping index Ω_E is calculated from gap size distributions determined from TRAC measurements; the woody-to-total area and needle-to-shoot area ratios are calculated from a combination of field and laboratory methods.

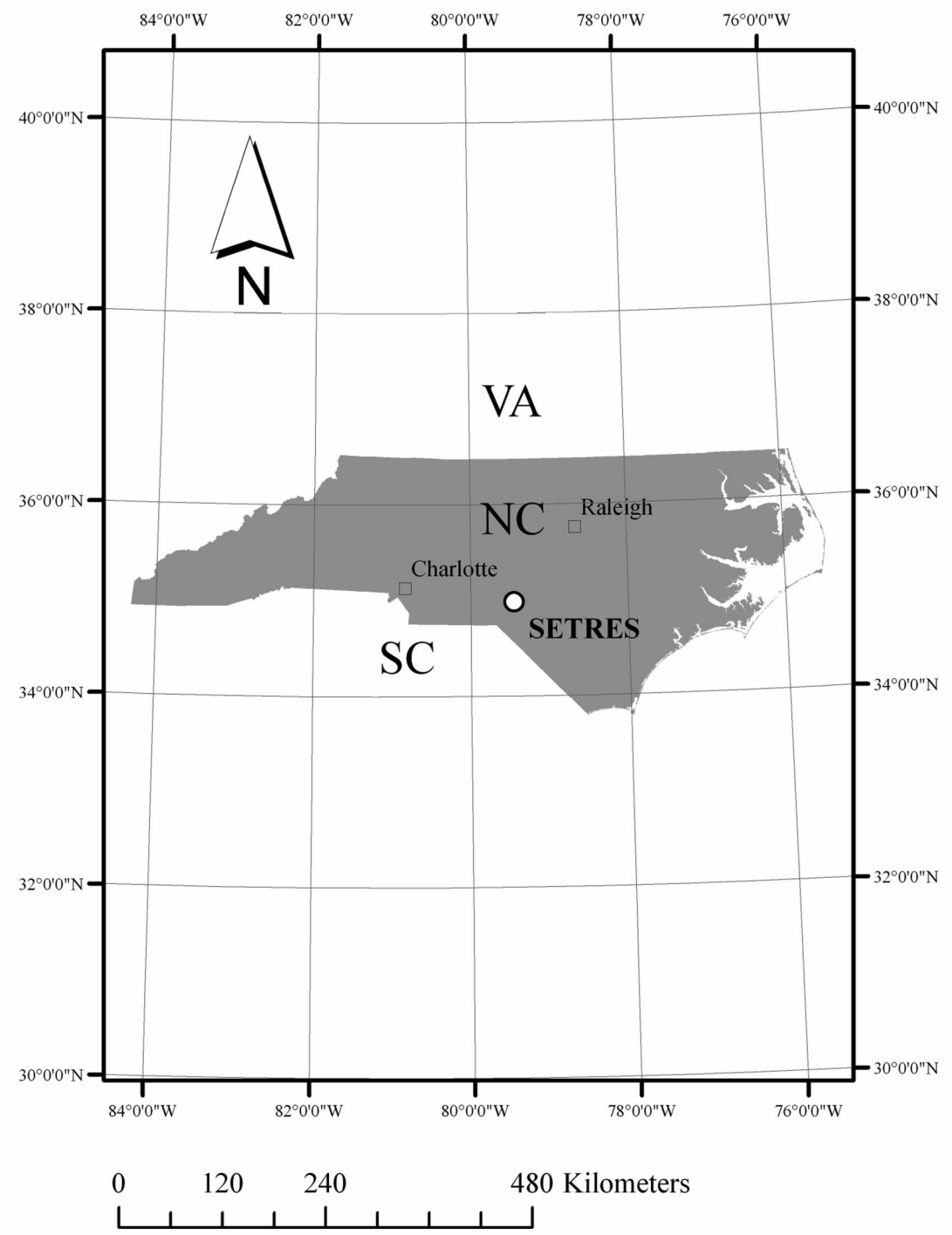

Figure 1. Location map of SETRES site in North Carolina.

TRAC and DHP Measurements

TRAC measurements were made at the SETRES site on Aug. 8, 2003 between 11:15 am and 4:43 pm, Eastern Standard Time (EST). Meteorological information obtained from the KSOP Moore County Airport weather station (35.237°N, 79.391°W) for that date and time period showed a relative humidity of 59–62%, a temperature of 84–86°C, visibility of 11.3 km, and cloud conditions ranging from few-to-scattered for level 1 clouds at an altitude of 1,097–1,189 m and broken-to-few for level 2 clouds at an altitude of 1,372–1,463 m.

Four TRAC runs were made along transect 2 (45° azimuth) between 11:16 am and 12:08 pm (EST). The θ ranged from 34.8 to 26.1° and the solar azimuth changed from 116.9 to 135.1° during this time interval. The PPFD was measured at a minimum/maximum of 1,150 μmol $(m^2)^{-1}$ s^{-1} and 1,684 μmol $(m^2)^{-1}$ s^{-1}, respectively, with magnitudes coinciding with increasing cloud cover (i.e., lower PPFD with increased crown cover). Transect 3 (90° azimuth) was run twice between 2:03 and 2:14 pm (EST) at a solar azimuth and θ of 206.7 and 21.9°, respectively. PPFD was measured at 1,772 μmol $(m^2)^{-1}$ s^{-1}. The last TRAC

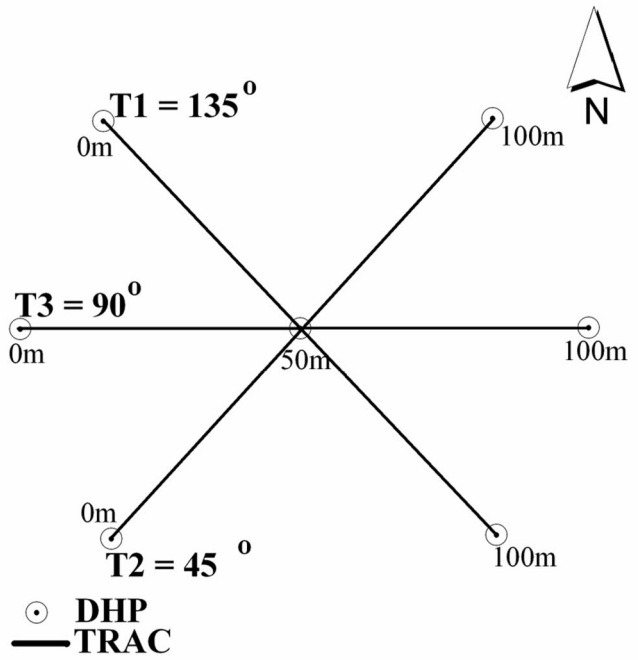

Figure 2. Plot design for SETRES S1P and S2P.

measurements were made on transect 1 (135° azimuth) between 3:08 and 4:43 pm (EST. Ranges for the θ and the solar azimuth were 30.8–48.9° and 236.2–258.9°, respectively. PPFD was measured at a minimum/maximum of 1,082 and 1,452 μmol $(m^2)^{-1}$ s^{-1}, respectively.

DHP measurements were made with a Nikon CoolPix 995 digital camera with a Nikon FC-E8 fisheye converter in diffuse light conditions. An image size of 1,600 × 1,200 pixels was selected at an automatic exposure. The camera was mounted on a tripod and leveled over each stake at a height of 1.4 m. The camera was leveled through the combination of two bubble levelers, one on the tripod and one mounted on the lens cap. Proper leveling of the instrument ensured that the "true" horizon of the photograph was captured. The camera was oriented to true north to compare metrics derived from other canopy gap instruments (i.e., TRAC, densitometer, and more). The operator selected a delayed exposure (i.e., 3–10 seconds) to offset any vibration incurred when depressing the shutter.

On Aug. 12, 2003, 19 DHPs were imaged on both plots (S1P and S2P), each image taken every 20 m along all three transects. The effective LAI (L_e) was determined from the processing of the DHPs using GLA software. After downloading the images, a GLA configuration file was created for the SETRES site. A configuration file contains information regarding image orientation, projection distortion and lens calibration, site location coordinates, length of growing season, sky-region brightness, and atmospheric conditions. GLA requires that each image be registered with respect to the location of due north on the image and the image circular area. This image registration required that the FC-E8 fisheye lens be recalibrated because of an actual field of view of 185°, not 180°. The image radius was reduced accordingly so that the 90° zenith angle represented the true horizon. After the image was registered, an analyst-derived threshold value was determined between sky (white pixels) and no sky (black pixels). The GLA software outputs L_e values at the fourth ring (0–60°) and the fifth ring (0–75°). To assume a projection coefficient of 0.5, L_e should be solved from a gap fraction determined at 57.3°. This can be done in GLA where gap fraction data are returned for the following zenith values: 5.6, 16.9, 28.1, 39.4, 50.6, 61.9, 73.1, and 84.4°. Then, the gap fraction at 57.3° can be determined by plotting gap fraction values against the corresponding zenith angle. Solving for L_e from the Beer-Lambert equation results in

$$L_e = \ln P(\theta)[-2\cos(\theta)], \quad (5)$$

where $P(\theta)$ is the gap fraction at zenith angle θ.

Needle-to-Shoot Ratio (γ_E)

The needle-to-shoot area ratios were measured from samples taken from the SETRES site and one other NCFNC site in south central Virginia. The needle-to-shoot area ratio was obtained through laboratory analysis of shoot samples following the methods of Chen and Black (1992a, 1992b) and Fassnacht et al. (1994). Three trees in the dominant canopy crown class were randomly selected from both sites. Within each tree, four shoot samples were taken from the lower, middle, and upper sections of each crown. Shoots were defined as the combination of the prior and current year needle growth. Therefore, one sampled tree yielded 12 shoot samples. Samples were hydrated and cooled to retain leaf moisture and then transported back to the laboratory for analysis.

In the laboratory, images of discrete shoot projections used to derive one-half total shoot area (A_s) were captured using an apparatus designed to facilitate multiple angle imaging (Fassnacht et al. 1994). Chen (1996) defined A_s as

$$A_s = 2 \cdot \frac{A_p(\theta, \Phi)\cos(15°) + A_p(\theta, \Phi)\cos(45°) + A_p(\theta, \Phi)\cos 75°}{\cos(15°) + \cos(45°) + \cos(75°)}, \quad (6)$$

where θ is defined as the camera incident angle (i.e., the camera angle from vertical) between the surface on which the shoot main axis rests (i.e., light table) and the camera direction, and φ is the azimuth angle of the shoot main axis with respect to any reference azimuth angle. The term $A_p(\theta, \Phi)$ is the projected area at θ and Φ. Digital images were taken at 15, 45, and 75° with a DSC S85 CyberShot camera (Sony, San Diego, CA) at 72 dots per inch (dpi) and then processed for shoot silhouette area (centimeters squared) with Image Tool 3.00 software, developed by the University of Texas Health Science in San Antonio (UTHSCSA 2002). The Image Tool 3.00 was calibrated by placing a 1-cm cut tab on the shoot's main axis.

After processing the shoots for A_s, one-half of the needle area per shoot (A_n) was estimated using the formula,

$$A_n = x\sqrt{VnL}/2, \quad (7)$$

where x is the loblolly shape factor, V is the volume of needles displaced (centimeters cubed), n is the number of needles on a shoot, and L is the average length of the needles (centimeters). Needles within each shoot were first counted to solve for n. In solving for V, the volume displacement method was implemented. This method is based on the principle that 1 ml of displaced water translates to 1 cm^3. For this technique, the entire shoot including the stem was immersed in an Erlenmeyer flask, without touching the bottom or the sides of the container. The displaced water volume was measured due to equal water exertion on all sides of the flask. The displaced volume of the needles was then determined by removing the needles

and then measuring the displaced volume of the stem. Subtracting the needles and stem-displaced volume from the displaced volume of the stem only resulted in the needle displacement volume. After finding *V*, 15 needles were randomly selected from each shoot and measured (centimeters) to give *L*. The loblolly shape factor is a dimensionless unit of measure, defined as the ratio of the perimeter (centimeters) of a needle cross-section to the square root of the cross-sectional area,

$$\text{shape factor} = \frac{\text{perimeter (cm)}}{\sqrt{\text{area (cm}^2\text{)}}} \quad (8)$$

(provided by M. Goyea, unpublished data, 1993). Duke University Nicholas School of the Environment provided four digital cross-sectional loblolly slides sampled from the bottom and the top of two trees from the Duke Free Air CO_2 Enrichment (FACE) Site (35.9,667°N, 79.0833°W). Area and perimeter measurements were made using Image Tool 3.00 software (UTHSCSA 2002).

A linear mixed-effects model was used to test for differences of γ_E means by site. This model allows for the inclusion of additional random effect terms and is appropriate for representing dependent data arising when observations are taken on related individuals (trees; Fox 2002). The basic model structure is

$$\mathbf{y}_i = X_i\beta + Z_i b_o + \varepsilon_i, \quad I = 1, \ldots, M,$$

$$b_i \sim \mathrm{N}(\mathbf{0}, \Psi),$$

$$\varepsilon_i \sim \mathrm{N}(\mathbf{0}, \sigma^2 I),$$

where the data are divided into *M* groups each with data vector $\mathbf{y}_i$; $\boldsymbol{\beta}$ is the vector of fixed effects; $\mathbf{b}_i$ is a vector of random effects ($\boldsymbol{\Psi}$ its unknown covariance matrix); $\boldsymbol{\varepsilon}_i$ is the vector of "within-group errors" and $\mathbf{X}_i$ and $\mathbf{Z}_i$ are the (known) fixed effects and random effects regressor matrices.

Woody-to-Total Area Ratio (α)

The woody-to-total area ratio accounts for the percentage of woody material contributing to the calculation of gap fraction. The woody-to-total area ratio was determined through a combined analysis approach isolating and retrieving the surface area measurement of the main stem area with ImageTool 3.00, and then analyzing the main canopy with Leica Imagine 8.6 software using an unsupervised clustering algorithm, the Iterative Self-Organizing Data Analysis Technique (ISODATA, Leica Image 8.6, Leica Geosystems, Heerbrugg, Switzerland) (Tou and Gonzales 1974). Four trees were selected from both plots for analysis. Selection criteria included relative isolation of the tree of interest, thus reducing vegetation overlap with neighboring canopies. Lateral images were taken with a Sony Digital Cyber-Shot DSC-S85 at 96-dpi resolution. Images were brought into ImageTool, calibrated, and then the areas of both the main stem and the canopy were computed through on-screen digitization. The main canopy image was clipped and imported as a TIFF (tagged image file format) image into Leica Imagine 8.6 software and the ISODATA clustering algorithm was used to separate green vegetation from the sky. This algorithm uses a minimum spectral distance to assign a cluster for each candidate pixel (ERDAS 1997). Arbitrary cluster means are specified at the initiation of the process and then multiple iterations shift the cluster means in the data. Initial parameters using 1 SD, 99% convergence, 20 classes, and a maximum of 10 iterations were input into the algorithm. In choosing ±1 SD from the mean, a total of 33% of the variation was initially assigned to classes 1 and 20. Because of the large variation ascribed to these two classes, the ISODATA algorithm splits and merges these classes over all the iterations. The percent of green vegetation identified from the ISODATA analysis was simply multiplied to the upper crown area computed earlier, to calculate a percent needle area.

Reference Stand-Level LAI: SETRES

Evaluation of the TRAC–DHP indirect optical technique for estimating stand-level LAI required a comparison to an assumed "truth" baseline. The NCFNC provided reference estimated stand-level LAI for the SETRES (day of the year [DOY] 224) site from a point-in-time estimation technique developed by Sampson et al. (2003). In a perfect scenario, reference stand-level LAI would be obtained by a complete harvest and measurement of every needle at the time of the indirect optical measurements. This would provide the most accurate evaluation of the TRAC–DHP method for estimating LAI. Practically, however, this method was not feasible. Therefore, an alternate means was needed to estimate stand-level LAI from destructive harvest data acquired at different periods of time from the indirect optical measurements. A summary of the Sampson method is as follows: (1) acquire 3 years of January stand-level foliage biomass (grams per hectare) from age- and treatment-specific whole-tree regression equations, (2) convert January stand-level foliage biomass (grams per hectare) to January stand-level LAI from year-specific January estimates of specific leaf area (SLA; centimeters squared per gram), and (3) determine stand-level LAI at the time period of interest by applying relative corrections for needle accretion and abscission.

Stand-level foliage biomass (grams per hectare) was estimated on both sites for 3 years of data corresponding to the current year (2003) and the two preceding years (2001 and 2002) for the month of January. Forest biometric measurements (dbh and height) were made for every tree by NCFNC at SETRES (four control plots; January 2001–2003). January stand-level foliage biomass was estimated with the aforementioned biometric measurements from age- and treatment-specific whole-tree regression equations developed at the SETRES location following the methods presented in Albaugh et al. (1998, 2004) These site- and plot-specific regression equations were based on destructive harvests from multiple years (i.e., 1992, 1994, 1996, 1998, and 2003) and included tree diameter and height as independent variables (Albaugh et al. 2005). After estimating 3 years of January stand-level foliage biomass (grams per hectare), an SLA conversion was applied to each year's data to yield a January stand-level LAI estimate. To arrive at stand-level LAI for the SETRES (DOY 224), modeled needle accretion and abscission were applied to each years stand-level LAI (2001–2003).

TRAC–DHP derived LAI is one-half the total green leaf area per unit ground surface area, or hemisurface area (HAS; Chen and Black 1992a). In contrast, LAI derived from the NCSFNC destructive harvests is the projected area of leaves including individual leaf inclinations. To permit direct comparison, a conversion factor was applied to transform HSA LAI to projected LAI. The projected area of a multisided needle is generally smaller than the HSA. The conversion factor was calculated through the analysis of the four cross-sectional loblolly slides provided by the Duke University Nicholas School of the Environment. Four main projection axes were measured using ImageTool 3.0 for each of the four needle cross-sections (Figure 3). For each of the four projection axis, a ratio of the length of the projection axis to one-half the perimeter was measured and

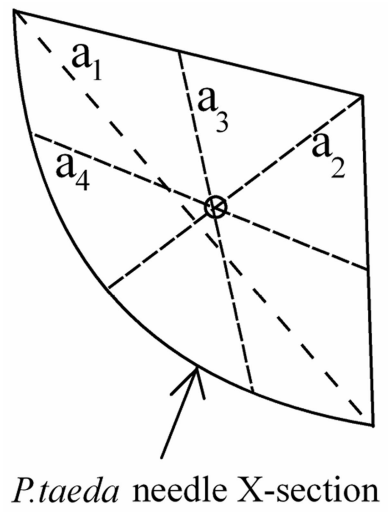

Figure 3. Main axes measured to determine HSA-to-projected conversion factor.

averaged to yield one conversion factor. The conversion factor determined from this method was 0.58 ($\sigma \pm 0.02$).

Alternative LAI Estimation Methods

We also calculated projected LAI using (1) DHP only (DHP methodology, Leblanc et al. 2005) and (2) TRAC processing only. DHP software, developed at the Canadian Centre for Remote Sensing, Quebec, Canada, retrieved the foliage element clumping index over a wide range of view zenith angles using the accumulated gap size distribution theory developed for the TRAC by Chen and Cihlar (1995a). LAI processed from TRAC alone assumed a random foliage distribution to solve for L_e.

Results

Element Clumping Index (Ω_E) and Effective LAI (L_e)

Element clumping index (Ω_E) measured at SETRES plot S1P was averaged over five TRAC runs of 100 m over all three transects ($n = 5$). The mean value of Ω_E was 0.89 ($\sigma \pm 0.03$) with a Ω_E range of 0.08. As a comparison, 10 60-m TRAC runs resulted in a mean Ω_E of 0.87 ($\sigma \pm 0.03$) with a Ω_E range of 0.11. Only the Ω_E values from the 100-m TRAC runs were used in the LAI calculations used to compare with LAI values from destructive harvests.

Effective LAI (L_e) was measured with DHP at the SETRES site on both plots S1P and S2P ($n = 20$/plot). These 20 L_e values per plot were averaged to return a mean L_e of 1.96 ($\sigma \pm 0.28$) and 1.97 ($\sigma \pm 0.29$), respectively. Ranges of L_e for the two plots were 0.97 (S1P) and 1.07 (S2P).

Needle-to-Shoot Area Ratio (γ_E)

The *P. taeda* shape factor, defined as the ratio of the perimeter (cm) to the area (cm^2) of a needle cross-section (Equation 8), had a mean value of 4.14 ($\sigma \pm 0.07$) with a range of 0.15. This value, in conjunction with the other field-measured parameters for γ_E calculation (Equation 8), yielded a needle area for 34 shoot samples across three trees, two at SETRES (S1P and S2P) and one at the south central Virginia site. The one-half shoot needle area (A_n) had a mean of 845.2 (cm^2) across all three plot means (samples/plot = plot mean), ranging from a plot mean minimum of 706.9 (cm^2) to a plot mean maximum of 976.4 (cm^2). The one-half shoot area (A_s) had a mean value of 745.7 (cm^2) across all three means, ranging from a plot mean minimum of 543.0 (cm^2) to a plot mean maximum of 1,000.4 (cm^2). Thus, the resulting needle-to-shoot area ratio (γ_E) had a mean value of 1.21 ($\sigma \pm 0.18$) across all three plots, ranging from a plot mean minimum of 1.00 to a plot mean maximum of 1.32.

Across all three plots, mean γ_E varied by crown position with the top portion of the canopy exhibiting the largest value ($\gamma_E = 1.62$). A linear mixed-effects model run in S-PLUS 2000 (Insightful Corp., Seattle, WA) showed that crown position was significant with respect to γ_E controlling for the random tree effect ($F = 12.99$; df = 2; $P < 0.05$). Based on an analysis of variance test ($F = 1.83$; df = 2; $P = 0.18$), the hypothesis that γ_E means by site were not significantly different was accepted.

Woody-to-Total Area Ratio (α)

A mean woody-to-total area ratio (α) value of 0.31 ($\sigma \pm 0.095$) was observed for four dominant *P. taeda* trees. The small crown branches contributed an average of 3.9% to the nonphotosynthetic portion of the trees as analyzed from the lateral image position.

TRAC–DHP-derived LAI

Parameter inputs required for LAI retrieval from the modified Beer-Lambert light extinction model (Equation 4) include: γ_E, Ω_E, L_e, and α (Table 1). Calculated TRAC–DHP HSA LAI was converted to a projected LAI of 1.06 for S1P and S2P.

Allometric Reference Stand-Level LAI

An LAI estimate for DOY 224 (2003) for the four control plots was 1.20 ($\sigma \pm 0.18$) with an LAI range of 0.41 (Table 2). First flush was initiated in early March with LAI decline beginning in early September (Figure 4).

Comparison of LAI Estimates

The TRAC–DHP indirect optical approach to estimating LAI performed well at the SETRES site where the allometric equations were developed (Table 3). Optical LAI estimates resulted in an LAI difference of 0.14 LAI units from destructive harvest-derived LAI. LAI estimated from DHP alone resulted in a smaller LAI differential (0.04) than the TRAC (0.77) and the TRAC–DHP (0.14).

Discussions and Conclusions

A number of LAI validation studies have used the integration of optical instruments to capture gap fraction measurements and gap size distributions to estimate L_e and Ω_E. Leblanc and Chen (2001) combined the TRAC with LiCOR PCA measurements for in situ LAI, as did Jonckheere et al. (2005). Recently, Ω_E has been extracted from gap size distribution within DHP measurements, potentially eliminating the need for TRAC measurements to obtain the same parameter (Leblanc et al. 2005). However, Chen et al. (2006) cautioned exclusive use of DHP to estimate Ω_E because of (1) the effect of multiple scattering causing a loss of leaf/needle resolution in the vertical direction and (2) the distortion of the gap size distribution resulting from the loss of these small gaps (Chen et al. 2006).

To date, no attempt has been made to quantify input measurements into the TRAC–DHP optical integrated technique to estimate LAI in *P. taeda* forest stands. Although the sample size for this study was small ($n = 1$), a good correlation existed between LAI derived from this technique and LAI retrieved from this site. An 11% underestimation of LAI via the TRAC–DHP method was

Table 1. Parameter inputs for TRAC–DHP integration calculation of leaf area index (LAI).

Site	Plot	γ_E	Ω_E	L_e	α	LAI (HSA)	LAI (projected)
SETRES	S1P	1.21	0.899	1.965	0.31	1.82	1.06
SETRES	S2P	1.21	0.899	1.975	0.31	1.83	1.06

Note: γ_E and α were measured in the field and analyzed in the laboratory; Ω_E (measured by TRAC) and L_e (measured by DHP); HSA conversion factor = 0.58.

Table 2. Control plot leaf area index (LAI) estimated from allometric equations derived from destructive harvest data at SETRES (2003).

Location	Plot	Year	Julian day	LAI
SETRES	1	2003	224	1.28
SETRES	2	2003	224	1.35
SETRES	3	2003	224	0.94
SETRES	4	2003	224	1.22
SETRES	Average			1.20

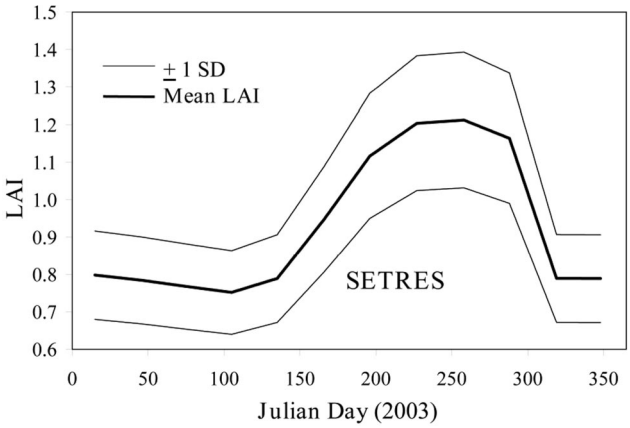

Figure 4. Seasonal leaf area index (LAI) derived from allometric equations based on destructive harvest data from SETRES (2003).

Table 3. TRAC–DHP: Allometric (ALLO) leaf area index (LAI) comparison.

LAI estimator	LAI	LAI difference*
ALLO	1.20	—
TRAC–DHP	1.06	−0.14
DHP	1.24	+0.04
TRAC	1.97	+0.77

* LAI difference is the difference between the allometrically derived LAI and the other three techniques.

observed at the SETRES site. Good correspondence can be attributed to reasonable estimates of the input parameters in Equation 4: woody-to-total area ratio (α), needle-to-shoot area ratio (γ_E), element clumping index (Ω_E), and effective LAI (L_e). The woody-to-total area ratio (α) estimate (0.31) was within the range of reported conifer (0.03–0.34) values from Gower et al. (1999). The needle-to-shoot area ratio (γ_E = 1.21) was also within reason with other reported values from the literature. Gower et al. (1999) reported a range of γ_E values from 1.2 (*Pinus banksiana*) to 2.08 (*Pinus resinosa*). In addition, the calculated shape factor for *P. taeda* of 4.14 was comparable with published values from Chen (1996): *P. banksiana* (4.00) and *Pinus mariana* (4.10). The element clumping index measured on both sites exhibited a narrower range than did with *P. banksiana* in the Canadian boreal ecotone (Chen 1996). *P. banksiana* varied by 0.18 Ω_E units (approximate) over the 30–45° θ range compared with a 0.10 Ω_E over the same 15° θ range from this study. Atmospheric conditions limited the time period for acquiring the Ω_E. Typical weather conditions at both sites included high relative humidity with increasing cloud cover throughout the day. Finally, the effective LAI acquired from DHP analysis resulted in a narrow range of variability at S1P and S2P ($\sigma \pm 0.28\ L_E$)

The needle-to-shoot factor has been noted as having the most variability of all the inputs to the modified Beer-Lambert light extinction model. The canopy architecture for *P. taeda* has significant variation due to indeterminate growth (multiple flushes) and high plasticity (i.e., developmental patterns) in foliage accretion and abscission in response to site fertility and drought (Sampson et al. 2003). With respect to the shape factor retrieved from the four needle cross-sections sampled from the Duke FACE site, enriched CO_2 has not been reported to change the cross-sectional needle dimensions. Rogers and Ellsworth (2002) did note, however, that no significant difference was detected for specific leaf mass between needles grown in ambient and elevated CO_2 conditions. Measurements of γ_E across a nutritional and moisture gradient will allow for site-specific inputs of this variable when using the TRAC–DHP method for LAI estimation.

DHP-processed LAI did provide an accurate estimate of LAI when compared with the whole-tree harvest (allometric) estimate at this one site. The benefits of this method over the combination method of TRAC–DHP would be that it eliminates the requirement for multiple instruments capturing different regimes of light attenuation. Using TRAC alone to estimate LAI might skew estimates above the actual values at the site.

The process of validating optically derived LAI from ground measurements requires the assumption of a comparative data layer of higher accuracy as "real truth," which, in this case, LAI derived from allometric equations developed from whole-tree harvests. However, both methods incur sampling and nonsampling error. The TRAC–DHP-integrated approach to optical LAI estimation has proved reliable on the SETRES site where the allometric equations for LAI estimation derived from whole-tree harvests were developed. Because of the documented variability existing within the *P. taeda* crown characteristics, added measurements of the needle-to-shoot area ratio (γ_E) and the woody-to-total area ratio (α) across multiple sites and ages would provide site-specific parameter inputs for Equation 4.

Literature Cited

ABER, J.D., AND J.M. MELILLO. 2001. *Terrestrial ecosystems.* San Diego, CA, Academic Press. 556 p.

ALBAUGH, T.J., H.L. ALLEN, P.M. DOUGHERTY, L.W. KRESS, AND J.S. KING. 1998. Leaf area and above- and belowground growth responses of loblolly pine to nutrient and water additions. *For. Sci.* 44:317–328.

ALBAUGH, T.J., H.L. ALLEN, P.M. DOUGHERTY, AND K.H. JOHNSEN. 2004. Long term growth responses of loblolly pine to optimal nutrient and water resource availability. *For. Ecol. Manag.* 192:3–19.

ALBAUGH, T.J., H.L. ALLEN, AND L.W. KRESS. 2005. Root and stem partitioning of *Pinus taeda. Trees-Struct. Funct.* 20(2):176–185.

BEER, A. 1853. *Einleitung in die höhere Optik*. Vieweg und Sohn, Braunschweig.

CHEN, J.M. 1996. Optically-based methods for measuring seasonal variation of leaf area index in boreal conifer stands. *Agric. For. Meteorol.* 80:135–163.

CHEN, J.M., AND T.A. BLACK. 1992a. Foliage area and architecture of plant canopies from sunfleck size distributions. *Agric. For. Meteorol.* 60:249–266.

Chen, J.M., and T.A. Black. 1992b. Defining leaf area index for non-flat leaves. *Plant Cell Environ.* 15:42l-429.

Chen, J.M., and J. Cihlar. 1995a. Quantifying the effect of canopy architecture on optical measurements of leaf area index using two gap size analysis methods. IEEE Geosci. *Remote Sens.* 33:777–787.

Chen, J.M., and J. Cihlar. 1995b. Plant canopy gap-size analysis theory for improving optical measurements of leaf-area index. *Appl. Optic.* 34:6211–6222.

Chen, J.M., and J. Cihlar. 1996. Retrieving leaf area index for boreal conifer forests using Landsat TM images. *Remote Sens. Environ.* 55:153–162.

Chen, J.M., P.M. Rich, S.T. Gower, J.M. Norman, and S. Plummer. 1997. Leaf area index of boreal forests: Theory, techniques, and measurements. *J. Geophys. Res.* 102:429–443.

Chen, J.M., A. Govind, O. Sonnentag, Y. Zhang, A. Barr, and B. Amiro. 2006. Leaf area index measurements at Fluxnet-Canada forest sites. *Agric. For. Meteorol.* 140:257–268.

Colomboa, R., D. Bellingerib, D. Fasolinic, and C.M. Marinob. 2003. Retrieval of leaf area index in different vegetation types using high resolution satellite data. *Remote Sens. Environ.* 86:120–131.

Cutini, A., G. Matteucci, and G.S. Mugnozza. 1998. Estimation of leaf area index with the Li-Cor LAI 2000 in deciduous forests. *For. Ecol. Manag.* 105:55–65.

Dougherty, P.M., L.H. Allen, L.W. Kress, R. Murthy, C. Maier, T.J. Albaugh, and D.A. Sampson. 1998. An investigation of the impacts of elevated carbon dioxide, irrigation, and fertilization on the physiology and growth of loblolly pine. P. 149–168 in *The productivity and sustainability of southern forest ecosystems in a changing environment*, Mickler, R.A., and S. Fox (eds.). Springer-Verlag, Berlin.

ERDAS. 1997. *ERDAS image field guide.* 4th ed. Atlanta. GA.

Fassnacht, K.S., S.T. Gower, J.M. Norman, and R.E. McMurtrie. 1994. A comparison of optical and direct methods for estimating foliage surface area index in forests. *Agric. For. Meteorol.* 71:183–207.

Fassnacht, K.S., and S.T. Gower. 1997. Interrelationships among the edaphic and stand characteristics, leaf area index, and aboveground net primary production of upland forest ecosystems in north central Wisconsin. *Can. J. For. Res.* 27:1058–1067.

Fassnacht, K.S., S.T. Gower, M.D. MacKenzie, E.V. Nordheim, and T.M. Lillesand. 1997. Estimating the leaf area index of north central Wisconsin forest using the Landsat Thematic Mapper. *Remote Sens. Environ.* 61:229–245.

Fournier, R.A., W. Mailly, J.N. Walter, and K. Soudani. 2003. Indirect measurement of forest canopy structure from in situ optical sensors. P. 77–114 in *Remote sensing of forest environments: Concepts and case studies,* Wulder, M.A., and S.E. Franklin (eds.). Kluwer Academic Publishers, Boston, MA.

Fox, J. 2002. *An R and S-Plus companion to applied regression.* Sage Publications, Thousand Oaks, CA. 294 p.

Geron, C.D., A.B. Guenther, and T.E. Pierce. 1994. An improved model for estimating emissions of volatile organic-compounds from forests in the eastern United-States. *J. Geophys. Res.* 99:12773–12791.

Gholz, H.L. 1982. Environmental limits on above-ground net primary production, leaf-area, and biomass in vegetation zones of the Pacific Northwest. *Ecology* 63:469–481.

Gottschalck, J.C., P.R. Houser, and X. Zeng. 2002. Impact of remotely sensed leaf area index on a Global Land Data Assimilation System. *Proc. of 16th conf. on Hydrology and the 13th symp. on Global change and climate variations*, Orlando, FL.

Gower, S.T., and J.M. Norman. 1991. Rapid estimation of leaf-area index in conifer and broad-leaf plantations. *Ecology* 72:1896–1900.

Gower, S.T., K.A. Vogt, and C.C. Grier. 1992. Carbon dynamics of Rocky-Mountain Douglas-fir—Influence of water and nutrient availability. *Ecol. Monogr.* 62:43–65.

Gower, S.T., C.J. Kucharik, and J.M. Norman. 1999. Direct and indirect estimation of leaf area index, fAPAR, and net primary production of terrestrial ecosystems. *Remote Sens. Environ.* 70:29–51.

Hall, R.J., D.P. Davidson, and D.R. Peddle. 2003. Ground and remote estimation of leaf area index in Rocky Mountain forest stands, Kananaskis Alberta. *Can. J. Remote Sens.* 29:411–427.

Johnsen, K.H., D. Wear, R. Oren, R.O. Teskey, F. Sanchez, R. Will, J. Butnor, D. Markewicz, D. Richter, T. Rials, H.L. Allen, J. Seiler, D. Ellsworth, C. Maier, L. Samuelson, G. Katul, and P. Dougherty. 2001. Meeting global policy commitments: Carbon sequestration and southern pine forests. *J. For.* 99:14–21.

Jonckheere, I., B. Muys, and P. Coppin. 2005. Allometry and evaluation of in situ optical LAI determination in Scots pine: a case study in Belgium. *Tree Phys.* 25:723–732.

Jones, H.G. 1992. *Plants and microclimate.* Cambridge University Press, Cambridge, MA. 433 p.

Kucharik, C.J., J.M. Norman, and S.T. Gower. 1998. Measurements of branch area and adjusting leaf area index indirect measurements. *Agric. For. Meteorol.* 91:69–88.

Leblanc, S.G., and J.M. Chen. 2001. A practical scheme for correcting multiple scattering effects on optical LAI measurements. *Agric. For. Meteorol.* 110:125–139.

Leblanc, S.G., J.M. Chen, and M. Kwong. 2002. *Tracing radiation and architecture of canopies. TRAC Manual, Ver. 2.1.3.* Natural Resources Canada, Canada Centre for Remote Sensing, Ottawa ON, Canada. 25 p.

Leblanc, S., J.M. Chen, R. Fernandes, D.W. Deering, and A. Conley. 2005. Methodology comparison for canopy structure parameters extraction from digital hemispherical photography in boreal forests. *Agric. For. Meteorol.* 129:187–207.

Leblanc, S.G., and R.A. Fournier. 2005. Towards a better understanding of in-situ canopy measurements used in the derivation and validation of remote sensing leaf area index products. P. 1–4 in *Proc. of conf. on International Symposium of Remote Sensing of Environment*, Saint Petersburg, Russia.

Leblanc, S.G., and J.H. Chapman. 2006. *Digital hemispherical photography manual.* Canada Centre for Remote Sensing, Quebec, Canada. 27 p.

Miller, J.B. 1967. A formula for average foliage density. *Aust. J. Bot.* 15:141–144.

Morisette, J.T., F. Baret, J.L. Privette, R.B. Myneni, J. Nickeson, S. Garrigues, N. Shabanov, M. Weiss, R. Fernandes, S. Leblanc, M. Kalacska, G. Sanchez-Azofeifa, M. Chubey, M.B. Rivard, P. Stenberg, M. Rautiainen, P. Voipio, T. Manninen, A. Pilant, T. Lewis, J. Iiames, R. Colombo, M. Meroni, L. Busetto, W. Cohen, D. Turner, E. Warner, G.W. Petersen, G. Seufert, and R. Cook. 2006. Validation of global moderate-resolution LAI Products: A framework proposed within the CEOS Land Product Validation subgroup. *IEEE Geosci. Remote Sens.* 44(7):1804–1817.

Murthy, R., and P.M. Dougherty. 1997. Effect of carbon dioxide, fertilization and irrigation on loblolly pine branch morphology. *Trees* 11(8):485–493.

Nilson, T. 1971. A theoretical analysis of the frequency of gaps in plant stands. *Agric. For. Meteorol.* 8:25–38.

Oren, R. C.I. Hsieh, P. Stoy, J. Albertson, H.R. McCarthy, P. Harrell, and G.G. Katul. 2006. Estimating the uncertainty in annual net ecosystem carbon exchange: Spatial variation in turbulent fluxes and sampling errors in eddy-covariance measurements. *Global Change Biol.* 12:883–896.

Rogers, A., and D.S. Ellsworth. 2002. Photosynthetic acclimation of *Pinus taeda* (loblolly pine) to long-term growth in elevated pCO_2 (FACE). *Plant Cell Environ.* 25:851–858.

Roxburgh, J.R., and D. Kelly. 1995. Uses and limitations of hemispherical photography for estimating forest light environments. *NZ J. Ecol.* 19:213–217.

Running, S.W., and J.C. Coughlan. 1988. A general-model of forest ecosystem processes for regional applications. 1. Hydrologic balance, canopy gas-exchange and primary production processes. *Ecol. Model.* 42:125–154.

Sampson, D.A., T.J. Albaugh, K.H. Johnsen, H.L. Allen, and S.J. Zarnoch. 2003. Monthly leaf area index estimates from point-in-time measurements and needle phenology for *Pinus taeda. Can. J. For. Res.* 33:2477–2490.

Schultz, R.P. 1997. *Loblolly pine: The ecology and culture of loblolly pine (*Pinus taeda *L.).* US For. Serv., Washington, DC. 493 p.

Smith, N.J., J.M. Chen, and T.A. Black. 1993. Effects of clumping on estimates of stand leaf area index using the LICOR LAI-2000. *Can. J. For. Res.* 23:1940–1943.

Soil Survey Division, NRCS, United States Department of Agriculture. 2001. *Official soil series descriptions.* USDA–NRCS Soil Survey Division. Available online at soils.usda.gov/technical/classified/osd/; last accessed Mar. 14, 2008.

Tian, Y., C.E. Woodcock, Y. Wang, J.L. Privette, N.V. Shabanov, L. Zhou, Y. Zhang, W. Buermann, J. Dong, B. Veikkanen, T. Hame, K. Andersson, M. Ozdogan, Y. Knyazikhin, and R.B. Myneni. 2002. Multiscale analysis and validation of the MODIS LAI product—II. Sampling strategy. *Remote Sens. Environ.* 83:431–441.

Tou, J.T., and R.C. Gonzalez. 1974. *Pattern recognition principles.* Addison-Wesley Publishing Co., Reading, MA.

University of Texas Health Science Center in San Antonio (UTHSCSA). 2002. *ImageTool 3.00 image processing and analysis program.* Available online at www.ddsdx.uthscsa/dig/itdesc.html; last accessed Mar. 14, 2008.

Weiss, M., L. Beaufort, F. Baret, D. Allard, N. Bruguier, and O. Marloie. 2001. *Mapping Leaf Area Index measurements at different scales for the validation of large swath satellite sensors: First results of the VALERI project*. Available online at www.avignon.inra.fr/valeri/documents/valeri-aussois.pdf; last accessed Mar. 14, 2008.

Wilson, W.J. 1963. Estimation of foliage denseness and foliage angle by inclined point quadrats. *Aust. J. Bot.* 11:95–105.